# 압축 응력 하에서의 콘크리트의 파괴거동

## Localizd Failure and Fracture Energies in Concrete under Compression

**최석환***

Choi, Sokhwan

ABSTRACT

The fracture behavior of high and normal strength concrete under compression was examined with specific controlling parameters such as strength of materials, length of specimens, end shear confinement, testing machine stiffness, and feedback signal. A servo-hydraulic closed-loop testing machine and a circumferential feedback signal were used to obtain a complete softening curve.

The use of friction-reducing materials introduced a limited failure zone with vertically oriented crack patterns and yielded a steeper slope in the softening curve. Additionally, the fracture energies with friction-reducing materials were much smaller than with high frictional confinement. Shorter specimens require a less fracture energy, meaning that the volumetric failure process is implied in the fracture rather than a single plane failure. Since localized deformations under compression can not be directly characterized as a material parameter, there is no unique stress-strain curve for concrete even with reduced end-confinement.

* 정회원, NSF Center for ACBM, post-doctoral fellow

• 본 논문에 대한 토의를 1998년 2월 30일까지 학회로 보내주시면 1998년 4월호에 토의회답을 게재하겠습니다.

Keywords : localization, softening, feedback signal, shear confinement, fracture energy, compression

## 1. Introduction

The failure processes of concrete under compression have not been satisfactorily understood due to the complication of compressive failure and the lack of precise experimental observations. High strength concrete has been broadly used in construction of high-rise buildings and bridges due to the benefits such as greater strength, stiffness, and durability. However, the material also has its disadvantage of being more brittle and exhibiting steeper post-peak behavior. Consequently, the understanding of the softening behavior of high strength concrete is even more essential for appropriate usage.

Microcracks coalesce each other to form a zone of damage when external loads are applied. The damaged zone is concentrated in a certain area after the peak load, and some parts of the specimen show unloading behavior. Strain softening refers to the response of concrete beyond the peak load, i.e. diminished load-carrying capacity. In order to utilize the softening branch in the design of concrete structures, better understanding of the strain softening processes is essential.

Recently researchers have recognized that the compressive failure in concrete is a localized behavior[1]. This finding drew close followings since the possibility of applying the fracture mechanics used to describe the tensile fracture behavior to the compressive fracture behavior becomes significant. Localization means that only a limited portion in a specimen carries all of the increasing strains. It implies that unloading process undergoes in other parts.

The failure localization and related fracture energies in concrete will be examined in conjunction with affecting testing conditions such as strength of materials, length of specimens, end shear confinement, testing machine stiffness, and feedback signal.

## 2. Experimental Program

Experiments under compressive loads are conducted on cylindrical concrete specimens which have different strengths and lengths. Mix proportions are given in Table 1. Natural aggregates with a maximum size of 10 mm were used. A superplasticizer (ASTM C-494 Type F, WRDA19) was used to achieve good workability of concrete with low water-cement ratio. The amount of superplasticizer for each

Table 1 Mix proportions(by weight)

| Batches | HSC | | | NSC | |
|---|---|---|---|---|---|
| Batch | 1 | 2 | 3 | 1 | 2 |
| Cement | 1.0 | 1.0 | 1.0 | 1.0 | 1.0 |
| Fine aggregate | 1.59 | 1.59 | 1.77 | 2.12 | 2.12 |
| Coarse aggregate | 1.96 | 1.96 | 2.18 | 2.61 | 2.61 |
| Microsilica fume slurry | 0.14 | 0.14 | 0.16 | - | - |
| Water | 0.34 | 0.34 | 0.21 | 0.56 | 0.58 |
| Superplasticizer(l/kg) | 0.01 | 0.01 | 0.02 | - | - |
| Water/cement ratio | 0.33 | 0.33 | 0.23 | 0.47 | 0.50 |

Water absorptions are 2.3% and 1.3% for fine and coarse aggregate, respectively.
Half of the microsilica fume slurry is water.
W/C ratio is based on saturated-dry condition of aggregates.

batch was slightly different based on the satisfactory workability at the mixing time. Three different lengths of specimens (100, 200, and 300 mm) were prepared with the same diameter of 100 mm. Specimens were placed in the water at a constant temperature of 20° C for 28 days after demolding. After 28 days, the specimens were placed in an environmental chamber with 50 % relative humidity and constant temperature of 20°C until the day of testing (8-9 weeks).

A digitally controlled servo hydraulic MTS with the capacity of 4.45MN was used.

## 2.1 End Loading Conditions

Since concrete and loading fixtures show different lateral expansions based on their Poisson's ratios, constraining shear friction will be generated between the two. The friction introduces tri-axial stress state near the contact area resulting in well-known conical failure. Ottosen[2] showed that significant axial stresses as well as large shear stresses exist along the edge of the specimen loading area. Various friction-reducing systems have been tried to reduce end shear confinement. Kotsovos[3] examined the behavior of concrete under different end conditions such as MGA pad, rubber layer, brush platen, and plain steel platen. It was shown that a complete and immediate loss of load-carrying capacity as soon as the maximum load is exceeded occurs in the post-peak behavior of concrete. A thin lubricant layer has also been used to reduce the frictional stresses. Some researchers have reported that the separate concrete blocks placed on top and bottom of a testing specimen provide smooth transition in restraint from the loading platen to the specimen[4].

The contact area between specimens and loading platens should be treated carefully, since it affects the displacement measurement and fracture behavior of the specimens. Capping compounds, a method used extensively for normal strength concrete (NSC), introduces soft layers and may change the final failure patterns[5]. In the current research, all specimens were ground until the maximum size of aggregates were exposed to the top and bottom loading surfaces. Then, three different end loading conditions were chosen for this study: (1) the bare steel platen case (DP); (2) a lubricant between a specimen and loading platens (LP). (The lubricant was a mixture of stearic acid and petroleum jelly) : Teflon (Polytetrafluorethylene, PTFE) sheets with the thickness of 50㎛ with the lubricant (TP).

## 2.2 Obtaining a Strain Softening Curve

There are several requirements in obtaining the descending portion of a load-displacement curve.

The stiffness of a testing machine is an important factor. The absolute value of the stiffness for the machine should be bigger than that of a specimen to overcome the stability problem in the post-peak range[6,7]. At the same time, a suitable feedback signal in conjunction with a closed-loop servo controlled testing machine is essential. The frequency response of the testing system should also be faster than the energy release rate of a specimen. Otherwise, unstable progress of failure can not be avoided[8].

To obtain the strength of a specimen, force control is sufficient as the feedback signal. However, if the post-peak behavior is desired, feedback signals that continuously increase in the post-peak range is required.

For normal strength concrete, the axial deformation can be used to control the whole fracture test. The cases that show very steep load-displacement curves or snap-back phenomenon in the post-peak range are (1) high strength concrete (HSC), (2) normal strength concrete (NSC) tested with a friction-reducing materials, and (3) specimens with a large slenderness ratio. For these cases, axial deformation control snaps through at the snap-back portion. Unlike axial deformation, lateral expansion or circumferential displacement should be used for the feedback signal for these cases since it increases continuously even in descending branch[14]. Other than circumferential expansions, the combined feedback signal of axial deformation and force can be used. This is particularly effective with a noncircular shaped specimen when a circumferential gage can not be easily installed on the surface[9,10]. This signal is also useful when the location of localized failure is unpredictable in a longer specimen.

Two different feedback signals were used for controlling the current tests. For NSC, specimens which have the length to diameter ratio of 1 or 2 were tested with the axial deformation feedback signal obtained from four LVDTs (linear variable differential transformers) equally spaced around a specimen. Unlike an extensometer attached on the middle of a specimen, these four LVDTs are arranged to measure platen to platen displacements in order to ensure that gage readings are not affected by aggressive crack development in the post-peak range[11,12]. The initial slope in the elastic range of each stress-strain curve was shifted to pass the origin to compensate the excessive deformations induced by the settlement process occurred between a specimen and loading platens.

All other specimens were tested with the circumferential feedback signal.

## 2.3 Stiffness of Testing Frame and Fixtures

The stiffness of a test machine is estimated based on a model[13]. The testing system can be separated into two main components : (1) the specimen, and (2) testing machine and fixture. As shown in Fig. 1a, $k_m$ represents the machine stiffness which includes the deformations from columns, crosshead, fixtures, connections, and hydraulic systems. $k_{sp}$ represents the stiffness of a specimen obtained from the platen to platen displacement. $k_s$ denotes the stiffness computed from the 'stroke' measurement corresponding to the movement of the piston of the actuator. Machine deformations obtained by cyclic loading showed a non-linear elastic behavior (Fig. 1b, 1c). When a specimen with a higher strength was tested, a linear behavior was shown after about 500 kN(Fig. 1d). The slope of the '$\delta_s$-$\delta_{sp}$load' curve represents the stiffness of the machine. The stiffness of the testing machine was not constant, but it depends on the applied load level and showed a maximum value (Fig. 1e). The maximum stiffness for the current setup was about 3,250 kN/mm, a far less than the specification of the testing machine of 13,100 kN/mm. Nonetheless, it is not feasible to get a unique value for the machine stiffness due to the dependence of $k_m$ on the specimen sizes, the number of loading spacers, and the length of loaded portion in columns.

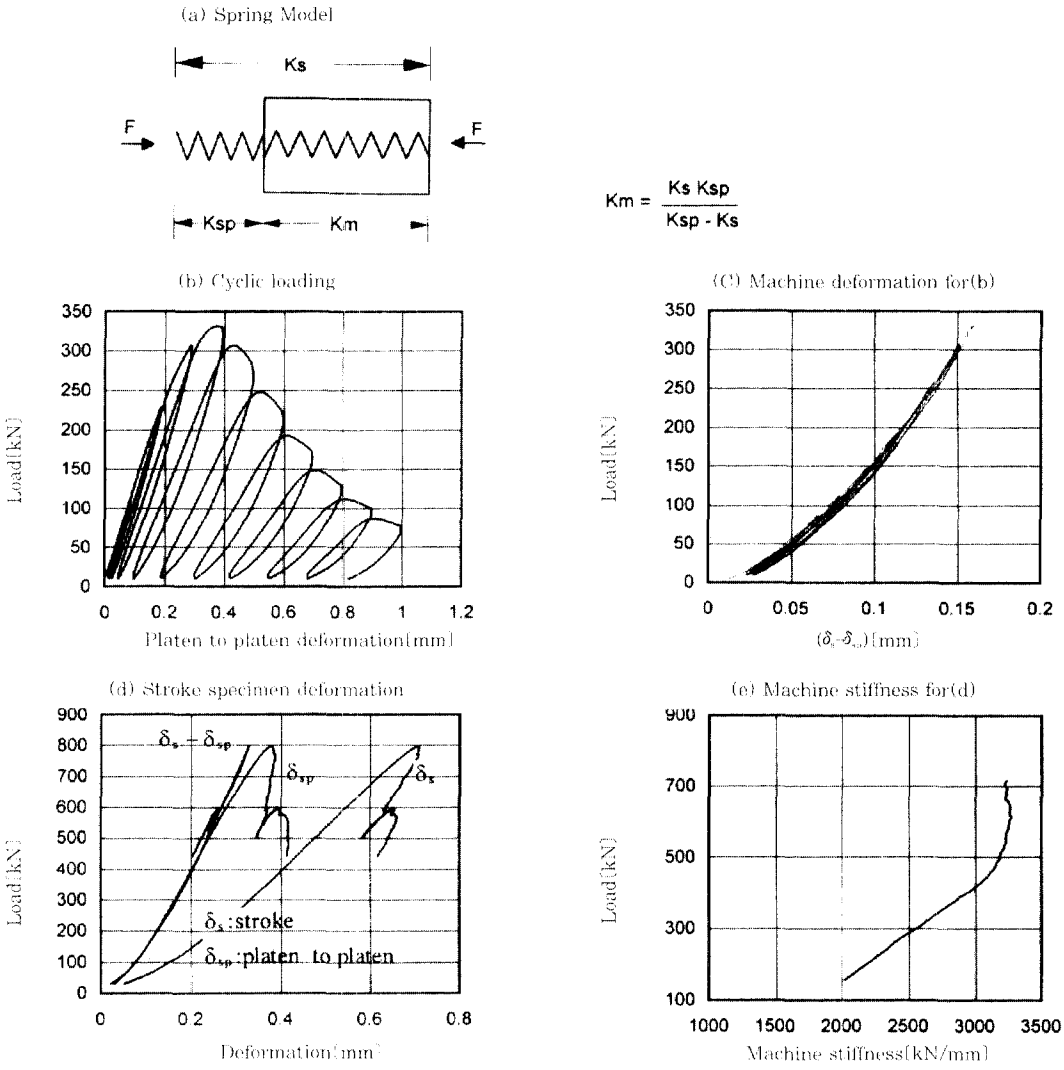


Fig. 1 Machine stiffness computation

## 3. Fracture Behavior of High and Normal Strength Concrete

The top loading platen was allowed to rotate to stabilize the sitting of the specimen. A rotating loading platen maintains moment equilibrium leading to a more uniformly applied stresses in all pieces, while a fixed loading platen supplies a uniform axial displacement giving higher stresses in some parts. Rotation of the loading platen is negligible in the pre-peak range but significant during the localization dominated in the post-peak range. In the post-peak range, the specimens tested with bare steel loading platens show less rotation than those tested with friction-reducing materials. In other words, the friction-reducing materials accelerate the localization of failure by removing end shear frictional constraint.

Peak stresses and peak strains for shorter specimens are significantly higher than

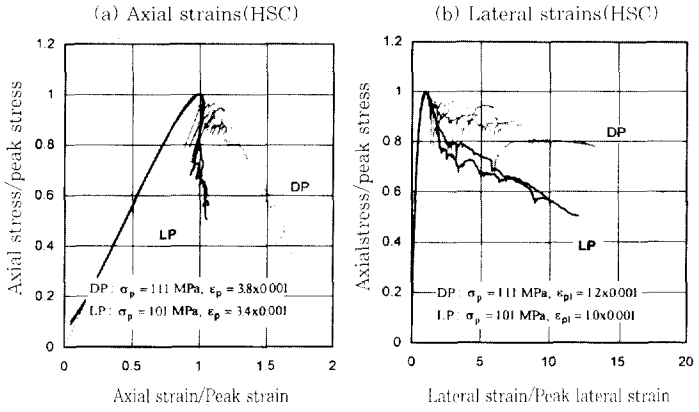


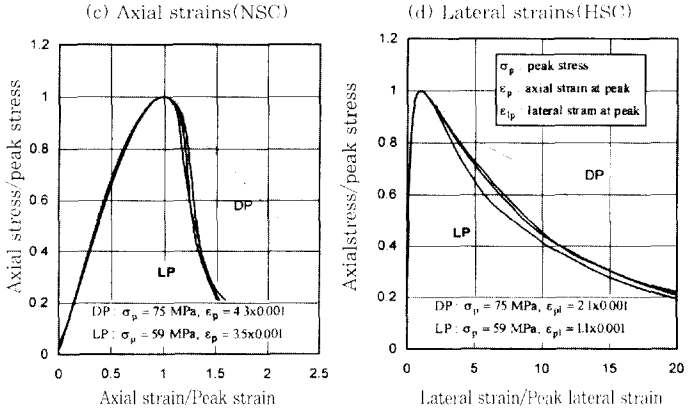


Fig. 2 Behavior of HSC and NSC (slenderness=1)

Fig. 3 Behavior of HSC for different specimen length(DP)

longer ones in both high and normal strength concrete. This trend was particularly obvious when DP was used.

The difference in peak stresses was about 20 % between slenderness=1 (75 MPa)(Fig. 2) and slenderness=2 (63MPa), while only a small difference existed between slenderness =2 and slenderness=3 (61 MPa). The peak strain decreased by about 40 % between slenderness=1 and slenderness=2. A further decrease of about 10 % was observed between slenderness=2 and slenderness=3. Longer specimens show steeper drop in their stress-strain curves since they have longer unloading zone. On the other hand, shorter specimens show more lateral strains at the same stress level by forming more macrocracks (HSC, DP; Fig. 3).

The specimens with slenderness=2 and slenderness=3 had similar crack patterns where no cracks formed on the loading surfaces due to the end confinement. These specimens expand considerably at the middle of the height and show the shear band. The crack pattern for slenderness=1 differs from the previous two cases. The lateral expansion at the middle does not dominate over the expansion at the top or bottom. Instead the vertical cracks are generally parallel to the loading axis.

It was observed that the vertical split

failure is combined with some inclined shear cracks. The loading surface is no longer intact even with DP, instead it formed cracks at the outer part of the loading zone.

It is a suitable observation that local tensile failure dominates the fracture when the shear confinement is removed (LP). The end condition changes the failure patterns and introduces larger crack openings at one portion of the specimen ends. This can be confirmed by final crack patterns on the loading surfaces (Fig. 4). The reason that cracks parallel to the loading axis do not form through the whole specimen length would be due to the material heterogeneity and imperfection of end loading conditions. When friction-reducing system is used, more cracks are developed in the middle portion of the loading surface. On the contrary, the number of cracks are reduced in high strength concrete and cracks are more concentrated on one portion of the loading area under the same end condition.

## 4. Localized Failure and Fracture Energies

Failure localization under tensile loading has been well described by separating single crack opening from the unloading portion. Under compression, the post-peak strains for longer specimens were less than those of shorter specimens. Even though this phenomenon is similar to that of a tensile specimen, it is more like a volumetric failure and not a hairline crack opening.

For the fracture energy computation, the stress versus localized deformation curve was linearly extrapolated at the end of measured data(Fig. 5). Fracture energy for the localized failure in the post-peak region can be represented as the area under the F-w curve in Fig. 5. The failure of concrete under high frictional confinement include shear bands and diffused tensile cracks requiring higher

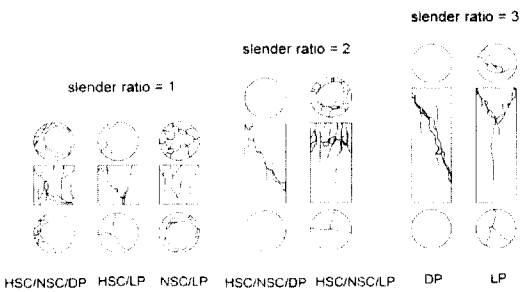

Fig. 4 Schematic drawings of failure patterns

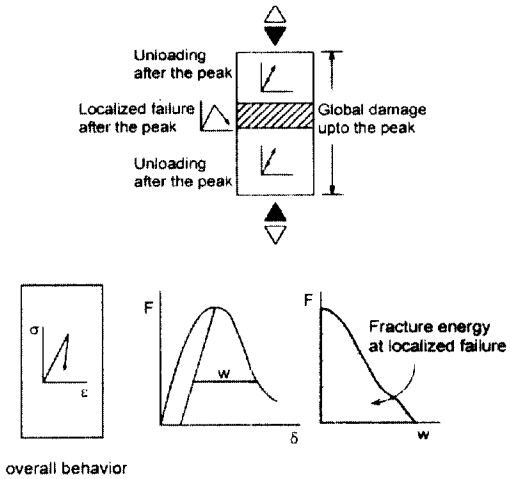

Fig. 5 Localized failure and fracture energy

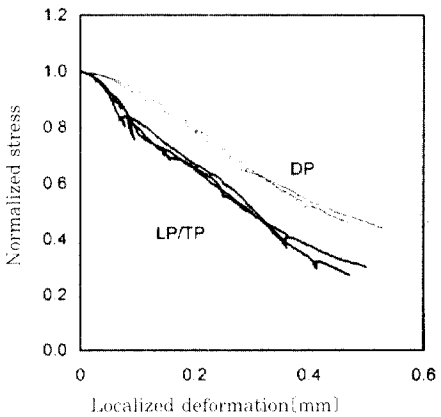

Fig. 6 Localized deformations under different end conditions (slenderness=2, HSC)

fracture energy than the one with friction-reducing materials (HSC, Fig. 6). The vertically oriented crack patterns shown in specimens with friction-reducing materials require less fracture energy.

The post-peak deformations exhibit a distinct trend based on the length of specimens as shown in Fig. 7. When the specimens are longer than certain length (slenderness=2, 3), the sizes of the fracture zone are similar to each other. Therefore, the post-peak displacements are independent of the specimen length.

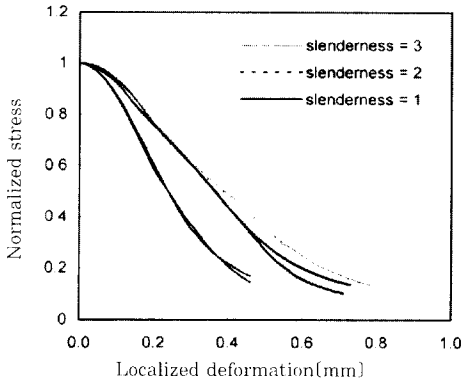


Fig. 7 Localized deformations for different slender ratios (LP, NSC)

Fracture energies related to the local tensile failure(LP) is much less than that of shear (or mixed) failure (DP) in all tested slender ratios. When the length of failure zone is longer than the length of a specimen, the specimen requires higher fracture energy (Fig. 8). When the slenderness is larger than 2, the specimen accommodates all major failure zone giving more or less constant fracture energy.

When friction-reducing materials are used, shorter specimens generated smaller fracture energies in both high and normal strength concrete. This is in contrast to the values obtained under DP. The load resistance of a specimen under LP may not be directly related to the localized fracture length itself under vertical crack patterns, and the longer specimens are able to form more cracks than the shorter one (slenderness=1).

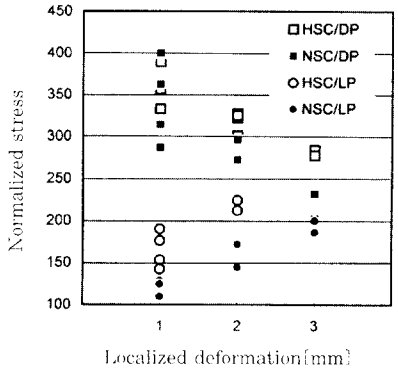


Fig. 8 Fracture energies under various conditions

## 5. Discussions and Conclusions

Localized failure always exists in concrete regardless of the end conditions. The use of friction-reducing materials introduced vertically oriented crack formation within a limited area in a specimen, and accelerated the failure process, and yielded a steeper slope of the descending branch. This phenomenon was more obvious for high strength concrete than for normal strength concrete.When the specimen was shorter than certain length (slenderness=1), it introduced mixed failure patterns (vertical split and shear band) under high shear confinement and vertical failure patterns under friction-reducing system. There is no unique stress-strain curve in concrete under compression even with a friction-reducing system.

Fracture energies required during the post-peak failure is much smaller when friction-reducing materials are used. The vertical tensile cracks formed under friction-

reducing materials require less energy to introduce the final failure in a specimen than shear band under high shear friction. Shorter specimens require less total fracture energies, meaning that the volumetric failure process is implied in the fracture not a single plane failure. As a consequence, localized deformations under compression can not be directly characterized as a material parameter but is affected by structural parameters.


### Acknowledgment

The financial support of the National Science Foundation Center for Science and Technology of Advanced Cement-Based Materials in United States is greatly appreciated.


## References


1. Van Mier, J. G. M., "Strain-softening of concrete under multiaxial loading conditions," Ph.D. thesis, Eindhoven University of Technology, the Netherlands, 1984
2. Ottosen, N. S., "Evaluation of concrete cylinder tests using finite elements," Journal of Engineering Mechanics, Vol. 110, No. 3, 1984, pp. 465-481
3. Kotsovos, M. D., "Effect of testing techniques on the post-ultimate behavior of concrete in compression," Materials and Structures, Vol. 16, No. 91, 1983, pp. 3-12
4. Shah, S. P., and Sankar, R., "Internal cracking and strain-softening response of concrete under uniaxial compression," ACI Materials Journal, Vol. 84, No. 3, 1987, pp. 200-212
5. Jansen, D., Shah, S. P., and Rossow, E., "Stress strain results of concrete from circumferential strain feedback control testing," ACI materials journal, Vol. 92, No. 4, 1995, pp. 419-428
6. Hudson, J. A., Crouch, S. L., and Fairhurst, C., "Soft, Stiff and Servo-Controlled Testing Machines: A Review with Reference to Rock Failure," Engineering Geology, Vol. 6, No. 3, 1972, pp. 155-189
7. Wang, F., Shah, S. P., and Naaman, A. E., "Stress-strain curves for normal and lightweight concrete in compression," Journal of American Concrete Institute, 1978, pp. 603-611
8. Hillerborg, A., "Stability problems in fracture mechanics testing," Fracture of Concrete and Rock : Recent Developments, ed. by S. P. Shah, S. E. Swartz and B. Barr, 1989, pp. 369-378
9. Okubo, S., and Nishimatsu, Y., "Uniaxial compression testing using a linear combination of stress and strain as the control variable," International Journal of Rock Mechanics and Mining Sciences & Geomechanics Abstracts, Vol. 22, No. 5, 1985, pp. 323-330
10. Glavind, M., and Stang, H., "Evaluation of the complete compressive stress-strain curve for high strength concrete," Fracture Processes in Concrete,Rock and Ceramics, RILEM, 1991, pp. 749-759
11. Choi, S., Thienel, K.-C., and Shah, S. P., "Strain softening of concrete in compression under different end constraints", Magazine of Concrete Research, 1996, Vol. 48, No. 175, June, pp. 103-115
12. J. G. M. van Mier et al., "Strain-softening of concrete in uniaxial compression," Materials and Structures, RILEM, Vol. 30, No. 198, May, 1997, pp. 195-209
13. Salamon, M. D. G., "Stability, Instability and Design of Pillar Workings," International Journal of Rock Mechanics and Mining, Vol. 7, No. 6, 1970, pp. 613-631



요 약

고강도 및 보통강도 콘크리트의 압축파괴 거동에 영향을 미치는 요소들(재료의 강도, 시편의 세장비, 전

단 구속, 실험장치의 강성, 피드백 신호)에 관한 연구가 수행되었다. 피드백 신호로 자동 조절되는 유압 실험기계 항에서 원주변형 피드백 신호를 사용하여 연화곡선을 구했다. 재하장치로 부터의 단부 전단 구속을 줄이면, 제한된 영역 안에서 재하방향 균형이 형성되고, 또한 연화곡선의 경사가 급해지고 파괴 에너지도 작아진다. 이때 길이가 큰 시편에서 파괴 에너지가 커지는 것은 안장과는 달리 단순균열이 형성되는 것이 아니고, 파괴가 용적을 가진다는 것을 의미한다. 압축응력하의 국부 파괴는 재료 특성이 아니므로, 단부 전단구속이 없더라도 재료적 특성으로서의 응력-변형도 곡선은 정하기 어렵다.

(접수일 : 1997. 5.16)